Electrochemical oxidation of *p*-chlorophenol on SnO_2–Sb_2O_5 based anodes for wastewater treatment

CARMEM L.P.S. ZANTA[1,]*, PIERRE-ALAN MICHAUD[2], CHRISTOS COMNINELLIS[2,]*
ADALGISA R. DE ANDRADE[3] and JULIEN. F.C. BOODTS[4]
[1]*Departamento de Química – CCEN, UFAL Maceió-Al, CEP 57072-970, Brazil*
[2]*Swiss Federal Institute of Technology, SB,ISP,1015-Lausanne, Switzerland*
[3]*Departamento de Química, FFCLRP-USP, Ribeirão Preto-SP, Brazil*
[4]*Instituto de Química, UFU, Uberlândia-MG, Brazil*
(*authors for correspondence, e-mails: clp@qui.ufal.br, christos.comninellis@epfl.ch)

Abstract

The influence of an IrO_2 interlayer between the Ti substrate and the SnO_2–Sb_2O_5 coating on the electrode service life and on the efficiency of *p*-chlorophenol (*p*-CP) oxidation for wastewater treatment has been investigated. The results have shown that if the loading of the SnO_2–Sb_2O_5 coating relative to the IrO_2 interlayer loading (γ ratio defined by Equation 1) is high ($\gamma = 20$–30) the service life of the electrode can be increased without modification of the ability of this electrode to perform *p*-CP oxidation. This suggests that the oxidation of *p*-CP using a Ti/IrO_2/SnO_2–Sb_2O_5 electrode with high γ ratio ($\gamma > 20$) occurs only through the SnO_2–Sb_2O_5 component of the electrode, with no interference of the IrO_2 interlayer. However, the electrode potential at a given current density is considerably lower in the case of the Ti/IrO_2/SnO_2–Sb_2O_5 electrode. In order to explain this decrease in electrode potential we speculate that water is firstly discharged on IrO_2, which is present in small amounts on the surface, forming hydroxyl radicals at a relatively low potential. These active hydroxyl radicals then migrate (spill over) towards the SnO_2–Sb_2O_5 coating, where they are physiosorbed and react with *p*-CP leading to complete combustion.

1. Introduction

Wastewater containing toxic or/and non-biodegradable organic pollutants, which cannot be easily treated through biological action, has to be treated using other techniques, usually chemical oxidation. Chemical oxidation, in general, allows complete elimination of the principal organic pollutants but complete removal of total organic carbon (TOC) is a difficult task. Thus oxidation of phenol with powerful oxidizing agents such as ozone ($E° = 2.07$) allows only a 30% TOC removal [1]. Similar levels of TOC removal are obtained using H_2O_2 in the presence of Fe^{2+} catalyst [2].

The electrochemical oxidation of organic compounds for wastewater treatment has attracted a great deal of attention [3–9] mainly because an appropriate choice of anode material can allow complete TOC elimination with high current efficiency. Typical examples of such materials are synthetic boron doped diamond (BDD) deposed on *p*-silicon substrate [9] and doped SnO_2–Sb_2O_5 coated on Ti base metal (Ti/SnO_2–Sb_2O_5) [4].

The main problem encountered with the BDD electrode is its high price and in the case of the Ti/SnO_2–Sb_2O_5 anode its low stability under anodic polarization.

In previous work [10] it was found that the presence of an IrO_2 interlayer between the Ti substrate and the SnO_2–Sb_2O_5 coating (Ti/IrO_2/SnO_2–Sb_2O_5) considerably increases the service life of the anode. This beneficial action of the IrO_2 interlayer was attributed to its high anodic stability and its isomorphous structure with TiO_2 and SnO_2 [10]. It was also found that the Ti/IrO_2/SnO_2–Sb_2O_5 electrode electrochemical activity for the oxygen evolution reaction (OER), lies between the Ti/IrO_2 and Ti/SnO_2–Sb_2O_5 electrodes due to the incorporation of IrO_2 in the SnO_2–Sb_2O_5 coating during electrode preparation [10].

The aim of this work is to investigate the influence of the IrO_2 interlayer between Ti and SnO_2–Sb_2O_5 coating (Ti/IrO_2/SnO_2–Sb_2O_5 electrode) on the anodic oxidation of organic compounds using *p*-clorophenol (*p*-CP) as a model compound.

2. Experimental details

The SnO_2–Sb_2O_5 based electrodes were prepared through the decomposition of the $SnCl_4 \cdot 5H_2O$ and $SbCl_3$ precursors in alcoholic solution, directly on Ti

(18 cm^2) or on Ti/IrO$_2$ support, using the spray pyrolysis technique. More details of the preparation of these electrodes using this technique are given elsewhere [10–12]. The Ti/IrO$_2$ support was prepared through deposition of IrO$_2$ on Ti using the thermal decomposition technique [13].

Cyclic voltammetry measurements were carried out using a three-electrode cell. Pt was used as the counter electrode, SnO$_2$–Sb$_2$O$_5$ based electrodes as the working electrode and Hg/Hg$_2$SO$_4$/K$_2$SO$_4$(sat) as reference. In order to increase the reproducibility of the polarization measurements, the electrodes were electrochemically preconditioned before use. The preconditioning consisted in polarizing the electrodes at 12 mA cm^{-2} for 2 h [4]. The working temperature was 25 °C.

A one compartment cell of 150 mL capacity was used in electrolysis experiments. The anode was an SnO$_2$–Sb$_2$O$_5$ based electrode and the cathode was a zirconium plate. Stirring was provided by a magnetic bar. A 1.0 mol l^{-1} Na$_2$SO$_4$ solution adjusted with H$_2$SO$_4$ to pH = 2 was used as supporting electrolyte. The working temperature was 30 °C. Electrolysis was carried out under galvanostatic conditions and the anode potential was measured during electrolysis using Hg/Hg$_2$SO$_4$/K$_2$SO$_4$(sat) as the reference electrode.

The disappearance of p-CP and the appearance of its oxidation products were monitored by HPLC (Shimadzu 8A). A Nucleosil C18 column was used with a mobile phase of acetonitrile/water 35/65 (v/v) at pH = 2 adjusted with addition of o-phosphoric acid at a flow rate of 0.8 ml min^{-1}. A UV detector (280 nm) was employed. The progress of the electrochemical oxidation was monitored by measuring the total organic carbon (TOC Shimadzu 5050) of the electrolysis solution.

3. Results and discussion

3.1. Electrochemical measurements

Cyclic voltammograms (CV) of the Ti/IrO$_2$/SnO$_2$–Sb$_2$O$_5$ electrodes containing different amounts of IrO$_2$ interlayer were obtained in 1.0 mol l^{-1} Na$_2$SO$_4$, adjusted with H$_2$SO$_4$ at pH = 2. The results were compared to those obtained with the Ti/IrO$_2$ and the Ti/SnO$_2$–Sb$_2$O$_5$ electrodes (Figure 1). The Ti/SnO$_2$–Sb$_2$O$_5$ electrode has a small voltammetric charge, in the potential region of water stability, in comparison with the Ti/IrO$_2$ electrode. The small voltammetric charge of the Ti/SnO$_2$–Sb$_2$O$_5$ electrode when compared to the Ti/IrO$_2$ electrode can be attributed to the low rugosity/porosity of the SnO$_2$–Sb$_2$O$_5$ coating [10] and the absence of surface redox transitions. This morphology is related to the preparation technique. In fact, the spray pyrolysis technique (used for the preparation of the SnO$_2$–Sb$_2$O$_5$ coating) favors the formation of crystalline and compact coatings [10] in contrast to the thermal decomposition technique (used for Ti/IrO$_2$ preparation) which favors the formation of a rough/porous coating [13].
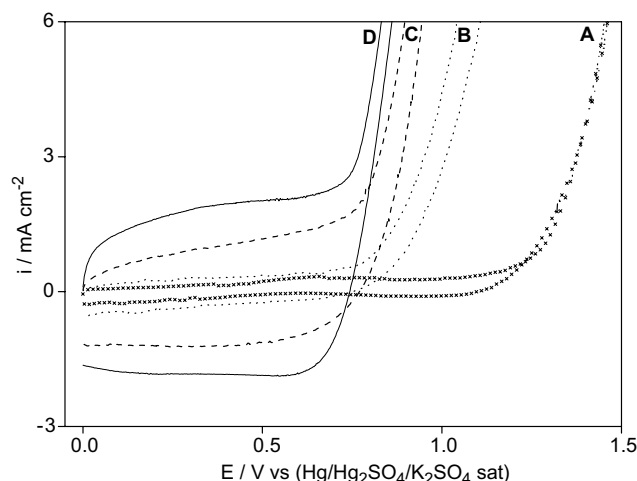

Fig. 1. Cyclic voltammograms obtained in 1.0 mol l^{-1} Na$_2$SO$_4$; pH = 2; T = 25 °C. (A) Ti/SnO$_2$–Sb$_2$O$_5$ (51 g m^{-2}); (B) Ti/IrO$_2$ (1.8 g m^{-2})/SnO$_2$–Sb$_2$O$_5$ (48 g m^{-2}); (C) Ti/IrO$_2$ (10 g m^{-2})/SnO$_2$–Sb$_2$O$_5$ (47 g m^{-2}); (D) Ti/IrO$_2$ (2.1 g m^{-2}).

Figure 1 clearly shows that in the presence of an IrO$_2$ interlayer (Ti/IrO$_2$/SnO$_2$–Sb$_2$O$_5$ electrode), the voltammetric charge increases with increasing IrO$_2$ interlayer loading. This contribution of IrO$_2$ to the voltammetric charge is certainly due to the incorporation of IrO$_2$ into the SnO$_2$–Sb$_2$O$_5$ coating by diffusion during the coating preparation.

Concerning the oxygen evolution reaction (OER) Figure 1 shows that the onset potential for this reaction on the Ti/SnO$_2$–Sb$_2$O$_5$ electrode is about 0.5 V higher than on the Ti/IrO$_2$ electrode. In the case of the Ti/IrO$_2$/SnO$_2$–Sb$_2$O$_5$ electrodes the onset potential for the OER is highly dependent on the amount of IrO$_2$ interlayer between the Ti substrate and the SnO$_2$–Sb$_2$O$_5$ coating. In other words, the thicker the IrO$_2$ interlayer, the lower is the onset potential for the OER. This is consistent with the proposal that IrO$_2$ is incorporated in the SnO$_2$–Sb$_2$O$_5$ during electrode preparation. In fact it seems that the amount of IrO$_2$ incorporated into the SnO$_2$–Sb$_2$O$_5$ coating and that reaches the coating surface increases with increasing IrO$_2$ interlayer loading, explaining satisfactorily the decrease in OER overpotential with increasing IrO$_2$ interlayer loading.

Figure 2 shows Tafel plots, corrected for ohmic drop that were obtained with the Ti/IrO$_2$/SnO$_2$–Sb$_2$O$_5$, Ti/SnO$_2$–Sb$_2$O$_5$ and Ti/IrO$_2$ electrodes in 0.5 mol l^{-1} H$_2$SO$_4$. The plots have a slope of 0.12 V dec^{-1} for all the investigated Ti/IrO$_2$/SnO$_2$–Sb$_2$O$_5$ electrodes, independently of the presence of the IrO$_2$ interlayer. However the Ti/IrO$_2$ electrode shows two linear potential regions with slopes of 0.07 and 0.12 V dec^{-1} at low and high current densities, respectively, in agreement with the value reported previously [13].

Polarization measurements in the presence of p-CP (2×10^{-2} mol l^{-1}) were obtained on both Ti/IrO$_2$ and Ti/IrO$_2$/SnO$_2$–Sb$_2$O$_5$ electrodes with different loadings of the IrO$_2$ interlayer (Figure 3). The presence of p-CP
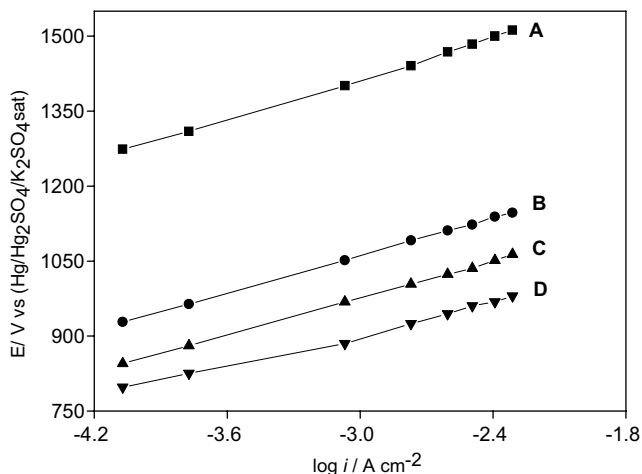
Fig. 2. Tafel plots for oxygen evolution reaction in 0.5 mol l^{-1} H$_2$SO$_4$; T = 25 °C. (A) Ti/SnO$_2$–Sb$_2$O$_5$ (30 g m^{-2}); (B) Ti/IrO$_2$ (10 g m^{-2})/SnO$_2$–Sb$_2$O$_5$ (30 g m^{-2}); (C) Ti/IrO$_2$ (10 g m^{-2})/SnO$_2$–Sb$_2$O$_5$ (10 g m^{-2}); (D) Ti/IrO$_2$ (10 g m^{-2}).
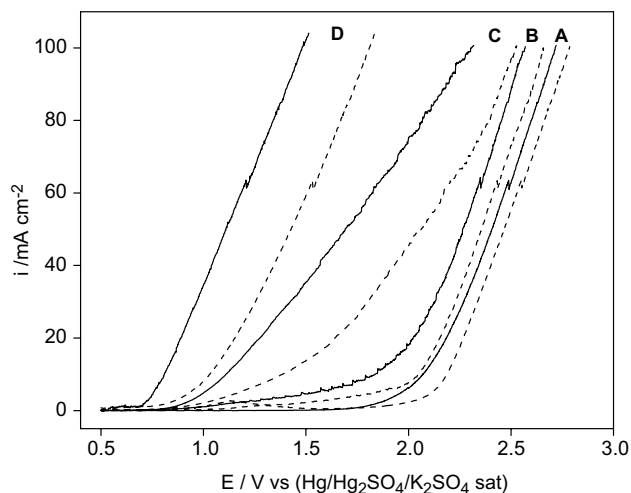
Fig. 3. Polarization curves in 1.0 mol l^{-1} Na$_2$SO$_4$, pH = 2, T = 25°C, in the absence (—) and presence (- - -) of 2 × 10^{-2} mol l^{-1} *p*-CP; scan rate: 10 mV s^{-1}. (A) Ti/SnO$_2$–Sb$_2$O$_5$ (51 g m^{-2}); (B) Ti/IrO$_2$ (1.8 g m^{-2})/SnO$_2$–Sb$_2$O$_5$ (48 g m^{-2}); (C) Ti/IrO$_2$ (10 g m^{-2})/SnO$_2$–Sb$_2$O$_5$ (47 g m^{-2}); (D) Ti/IrO$_2$ (2.1 g m^{-2}).

in the electrolyte deactivates all the investigated electrodes (decrease in current at a given potential). However, this deactivation seems to be sensitive to the IrO$_2$ interlayer loading. In fact it seems that the tendency of the electrode to be deactivated increases with increasing loading of the IrO$_2$ interlayer and consequently with the amount of IrO$_2$ incorporated into the SnO$_2$–Sb$_2$O$_5$ coating. Maximum deactivation is observed for a pure IrO$_2$ coating. Deactivation in the presence of organic compounds from electrodes rich in IrO$_2$ can be associated with the formation of a polymeric film on the electrode surface which blocks the active sites. The formation of this polymeric film also depends on the experimental conditions used. Therefore, alkaline media, low current density, high temperature and high *p*-CP concentration favors polymer film formation.

Similar behavior has been reported using Pt [14] and BDD [15] electrodes.

3.2. *Electrochemical oxidation of p-chlorophenol (p-CP)*

The anodic stability and the electrochemical behavior of the Ti/IrO$_2$/SnO$_2$–Sb$_2$O$_5$ electrodes toward *p*-CP oxidation (main reaction) and oxygen evolution (side reaction) strongly depends on the ratio between the SnO$_2$–Sb$_2$O$_5$ coating loading and the IrO$_2$ interlayer loading. This ratio has been defined as the γ ratio (Equation 1).

$$\gamma = \frac{\text{loading of SnO}_2 - \text{Sb}_2\text{O}_5 \text{ coating (g m}^{-2})}{\text{loading of IrO}_2 \text{ interlayer (g m}^{-2})} \quad (1)$$

High γ values increase the electrode service life, however, the efficiency of *p*-CP oxidation decreases with increasing γ values. In fact an optimum γ ratio must be used in order to achieve both high electrode service life and high *p*-CP oxidation efficiency. Preliminary measurements have shown that this optimum γ ratio lies between 20 and 30.

The anodic oxidation of *p*-CP has been investigated using two SnO$_2$–Sb$_2$O$_5$ based electrodes, one electrode without an IrO$_2$ interlayer (Ti/SnO$_2$–Sb$_2$O$_5$ electrode) and another electrode having an interlayer with a γ ratio equal to 26.6 [Ti/IrO$_2$ (1.8 g m^{-2})/SnO$_2$–Sb$_2$O$_5$ (48 g m^{-2}) electrode].

The anodic oxidation of a *p*-CP (2 × 10^{-2} mol l^{-1}) aqueous solution in 1.0 mol l^{-1} Na$_2$SO$_4$ was carried out at constant pH (pH = 2) and temperature (30 °C) under galvanostatic conditions (30 mA cm^{-2}). The evolution of the anode potential, *p*-CP concentration and TOC during the oxidation of *p*-CP is shown in Figure 4 for both electrodes. This figure shows that the presence of the IrO$_2$ interlayer decreases the electrode potential and allows operation at constant potential during almost all the process. This indicates a higher stability of the electrodic material. In fact the potential of the Ti/IrO$_2$/SnO$_2$–Sb$_2$O$_5$ electrode initially increases and, after the passage of an electrical charge (*Q*) of about 40 A h L^{-1}, it stabilizes at about 3 V. In the absence of an IrO$_2$ interlayer the situation is different. The anode potential of the Ti/SnO$_2$–Sb$_2$O$_5$ electrode firstly increases, stabilizing at 4.5 V before the passage of about 40 A h L^{-1}. For *Q* > 120 A h L^{-1} the electrode potential rapidly increases with *Q* indicating deactivation of the electrode.

The rate of *p*-CP oxidation and TOC elimination also depends strongly on *Q*. Two regions can be distinguished. For *Q* < 100 A h L^{-1} both electrodes behave similarly towards *p*-CP oxidation and TOC elimination (Figure 4A and B). However, for *Q* > 100 A h L^{-1}, the rate of TOC elimination at the Ti/IrO$_2$/SnO$_2$–Sb$_2$O$_5$ electrode is higher than at Ti/SnO$_2$–Sb$_2$O$_5$. The decrease in the rate of TOC elimination at the latter electrode material coincides with the onset of the increase in anode potential. This behavior suggests the beginning of electrode deactivation after the passage of about
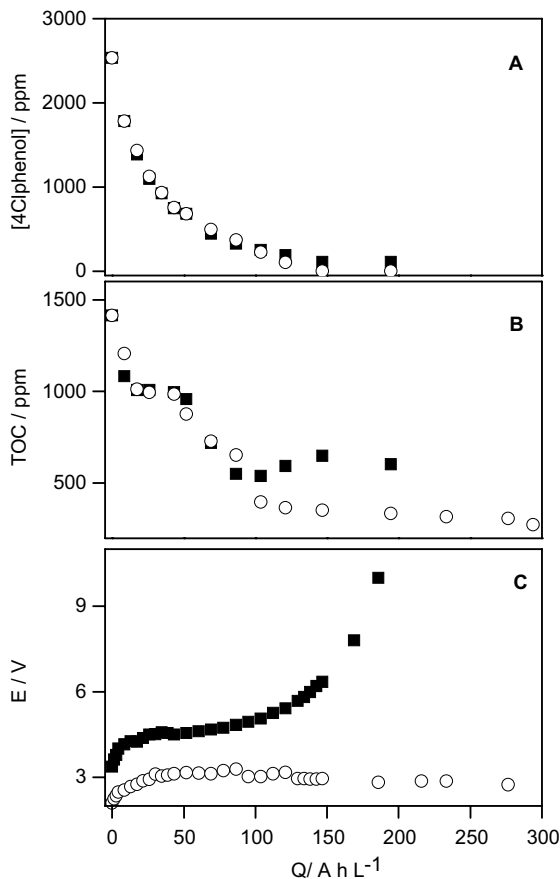
Fig. 4. (A) *p*-CP concentration, (B) TOC and (C) anode potential as a function of specific anodic charge (○) Ti/IrO$_2$/SnO$_2$–Sb$_2$O$_5$ and (■) Ti/SnO$_2$–Sb$_2$O$_5$. Conditions: $i = 30$ mA cm^{-2}, $T = 30$ °C
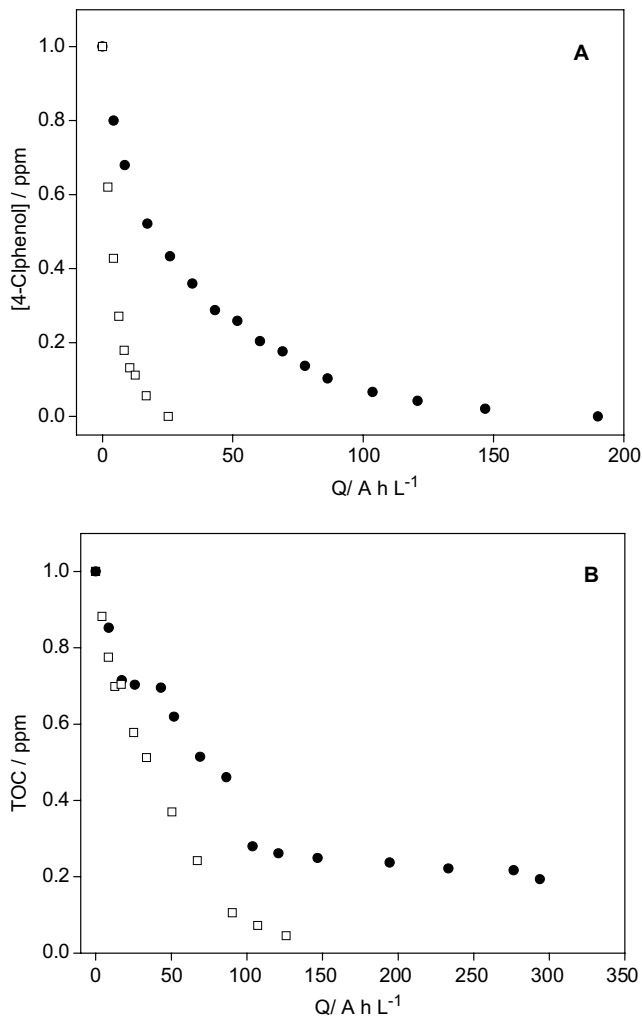

Fig. 5. Influence of initial *p*-CP concentration on the rate of: (A) *p*-CP oxidation; (B) TOC elimination at Ti/IrO$_2$/SnO$_2$/Sb$_2$O$_5$ electrode with $\gamma = 26.6$: (●) 20 mmol of *p*-CP l^{-1}; (□) 3.9 mmol l^{-1} of *p*-CP. Conditions: $i = 30$ mA cm^{-2}, $T = 30$ °C.

120 A h L^{-1}. The Ti/IrO$_2$/SnO$_2$–Sb$_2$O$_5$ electrode does not give any indication of deactivation during the experiment. The high stability of the Ti/IrO$_2$/SnO$_2$–Sb$_2$O$_5$ electrode has been previously reported by Correa-Lozano et al. [10].

It is worth mentioning that during the oxidation of *p*-CP, a yellow polymeric material was formed on the anode surface.

The influence of *p*-CP concentration on its oxidation rate and TOC elimination is shown in Figure 5. For dilute *p*-CP solution 95% TOC elimination can be achieved using the Ti/IrO$_2$/SnO$_2$–Sb$_2$O$_5$ electrode with a ratio between the SnO$_2$–Sb$_2$O$_5$ coating loading and the IrO$_2$ interlayer loading equal to 26.6 ($\gamma = 26.6$). For more concentrated *p*-CP solution, about 80% of TOC is eliminated. This shows the applicability of Ti/IrO$_2$/SnO$_2$–Sb$_2$O$_5$ electrodes in technological electrochemical treatment mainly for solutions containing low concentrations of hazardous compounds.

3.3. *General discussion*

It has been previously reported that IrO$_2$ in SnO$_2$–Sb$_2$O$_5$ based electrodes behaves differently toward O$_2$ evolution and organic oxidation [16]. At an SnO$_2$–Sb$_2$O$_5$ based anode, a non-active electrode, the oxidation of organic

compounds occurs through physiosorbed hydroxyl radicals generated from water oxidation. These active hydroxyl radicals can lead to the complete combustion of the organic compounds (step 5, Figure 6). At an IrO$_2$
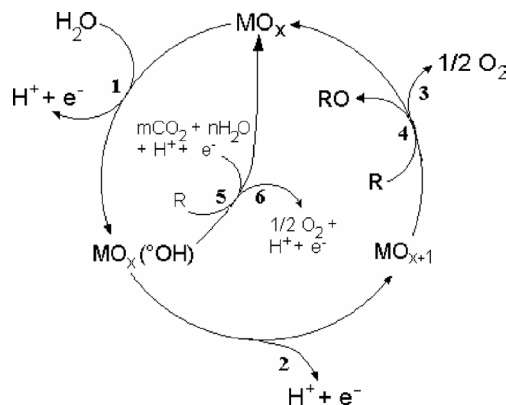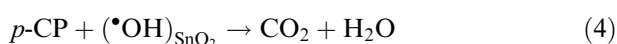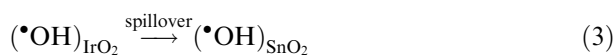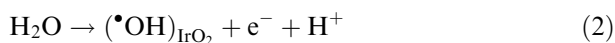

Fig. 6. Scheme of oxidation of organic compounds with simultaneous oxygen evolution at metal oxide anodes.

based anode, known as an active electrode, the reaction occurs through a higher oxidation state of the metal oxide surface sites, generally resulting in a partial oxidation of the organic compounds (step 4, Figure 6). It has also been demonstrated that the presence of an IrO_2 interlayer (Ti/IrO_2/SnO_2–Sb_2O_5 electrodes) strongly increases the electrode service life [10].

In this work we have shown that the activity of Ti/IrO_2/SnO_2–Sb_2O_5 electrodes toward the OER and p-CP oxidation lies between the results obtained with Ti/IrO_2 and the Ti/SnO_2–Sb_2O_5 electrodes. This is attributed to the incorporation of IrO_2 in the SnO_2–Sb_2O_5 coating during preparation. However, the effect of the IrO_2 interlayer in the SnO_2–Sb_2O_5 coating can be strongly decreased by increasing the loading of the SnO_2–Sb_2O_5 coating relative to the IrO_2 interlayer loading (γ ratio defined by Equation 1), i. e., $\gamma > 20$.

The fact that we did not observe a significant change in the behavior of p-CP oxidation using low loadings for the IrO_2 interlayer ($\gamma = 26$) suggests that p-CP oxidation at the Ti/IrO_2/SnO_2–Sb_2O_5 electrode occurs mainly through the SnO_2–Sb_2O_5 component. In other words, it occurs through physiosorbed hydroxyl radicals on SnO_2–Sb_2O_5. However, the electrode potential is considerably lower than in the case of Ti/SnO_2–Sb_2O_5 electrodes. In order to explain this decrease in electrode potential, one can speculate that $^\bullet$OH radicals formed on IrO_2 by primary water discharge (Equation 2) spill over toward SnO_2–Sb_2O_5 (Equation 3), were they are physiosorbed and react with p-CP (Equation 4) leading to complete combustion of the organic compound.

$$H_2O \rightarrow (^\bullet OH)_{IrO_2} + e^- + H^+ \quad (2)$$

$$(^\bullet OH)_{IrO_2} \xrightarrow{\text{spillover}} (^\bullet OH)_{SnO_2} \quad (3)$$

$$p\text{-CP} + (^\bullet OH)_{SnO_2} \rightarrow CO_2 + H_2O \quad (4)$$

4. Conclusion

The influence of an IrO_2 interlayer between the Ti substrate and the SnO_2–Sb_2O_5 coating on the anodic oxidation of p-CP has been investigated and the results have shown that:

(1) The presence of an IrO_2 interlayer strongly increases the service life of the Ti/SnO_2–Sb_2O_5 electrode due to its high anodic stability and its isomorphous structure with TiO_2 (formed on the Ti substrate).

(2) The voltammetric behavior indicates that incorporation of IrO_2 into the SnO_2–Sb_2O_5 coating occurs.

(3) If the loading of the SnO_2–Sb_2O_5 coating relative to the IrO_2 interlayer loading (γ ratio defined by Equation 1) is high ($\gamma = 20$–30) the service life of the electrode can be increased without significant affect on the ability of the electrode to carry out p-CP oxidation. This suggests that oxidation of p-CP at the Ti/IrO_2/SnO_2–Sb_2O_5 electrode with $\gamma = 20$–30 occurs only through the SnO_2–Sb_2O_5 component without any interference of the IrO_2 interlayer.

(4) More than 95% TOC elimination can be achieved during the treatment of dilute p-CP solutions using the Ti/IrO_2/SnO_2–Sb_2O_5 electrode with a γ ratio equal to 26.6.

References

1. G.L. Anderson, *AICHE Symp. Ser.* **73** (1977) 265.
2. N. Al-Hayek and S. Dore, *Environ. Tech. Lett.* **6** (1985) 37.
3. Ch. Comninellis and C. Pulgarin, *J. Appl. Electrochem.* **21** (1991) 703.
4. Ch. Comninellis and C. Pulgarin, *J. Appl. Electrochem.* **23** (1993) 1083.
5. Ch. Comninellis and A. Nerini, *J. Appl. Electrochem.* **25** (1995) 23.
6. A.M. Polcaro and S. Palmas, *Ind. Eng. Chem. Res.* **36** (1997) 1791.
7. O. Simond, V. Schaller and Ch. Comninellis, *Electrochim. Acta* **42** (1997) 2009.
8. A.M. Polcaro, S. Palmas, F. Renoldi and M. Mascia, *J. Appl. Electrochem.* **29** (1999) 147.
9. M. Panizza, P.-A. Michaud, G. Cerisola and Ch. Comninellis, *J. Electroanal. Chem.* **507** (2001) 206.
10. B. Correa-Lozano, Ch. Comninellis and A. De Battisti, *J. Appl. Electrochem.* **27** (1997) 970.
11. B. Correa-Lozano, Ch. Comninellis and A. De Battisti, *J. Appl. Electrochem.* **26** (1996) 683.
12. B. Correa-Lozano, Ch. Comninellis and A. De Battisti, *J. Electrochem. Soc.* **143** (1996) 203.
13. S. Trasatti, 'Electrodes of conductive mettalic oxides' Part A, in (Ed.) (Elsevier, Amsterdam, 1980).
14. J.D. Rodgers, W. Jedral and N.J. Bunce, *Environ. Sci. Technol.* **33** (1999) 1453.
15. M.A. Rodrigo, P.-A. Michaud, M. Paniza, G. Cerisola and Ch. Comninellis, *J. Electrochem. Soc.* **148** (2001) D60.
16. G. Fóti, D. Gandini and Ch. Comninellis, *Curr. Top. Electrochem.* **5** (1997) 71.